MEASUREMENTS OF TIME-SPACE DISTRIBUTION OF CONVECTIVE HEAT TRANSFER TO AIR USING A THIN CONDUCTIVE-FILM

Hajime Nakamura
Department of Mechanical Engineering,
National Defense Academy
1-10-20 Hashirimizu, Yokosuka, Kanagawa, 239-8686, Japan
nhajime@nda.ac.jp

ABSTRACT

A measurement technique of time-space characteristics of heat transfer to air has been developed using a thin conductive film and a high-speed infrared thermograph. In this work, a titanium foil of 2 μm thick was used as a test surface, and measured temperature on it by employing an infrared thermograph of 120 Hz. The accuracy of the measurements was confirmed by comparing the heat transfer coefficient of a laminar boundary layer to that of a numerical analysis. In order to verify the applicability of this measurement technique to practical measurements, unsteady heat transfer on the wall of a turbulent boundary layer was examined. It was possible to restore the time-space distribution of the heat transfer coefficient up to 30 Hz in time and 4.5 mm in spatial wavelength by solving the heat conduction equations inside the wall, even though the heat transfer coefficient was low ($\bar{h}$ = 10 – 20 W/m^{2}K). The results showed that the time-space behavior of the heat transfer was clearly revealed, which was reflected by the streaks formed in the near-wall region of the turbulent boundary layer. The statistical values of the turbulent boundary layer, that is, rms value of the fluctuating heat transfer coefficient and mean spacing of the thermal streaks, agreed well to those of previous data of DNS and experiments.

INTRODUCTION

Convective heat transfer generally has a nature of nonuniformity and unsteadiness, which is reflected by a three-dimensional flow near a wall. However, most experimental studies concerning the convective heat transfer have been performed in a time-averaged manner or using one-point measurements. This frequently results in poor understandings on the mechanisms of the heat transfer.

Measurement techniques for time-space characteristics of the heat transfer have been developed using liquid crystal (Iritani et al., 1983) or using infrared thermography (Hetsroni and Rozenblit, 1994, and Nakamura and Igarashi, 2004, 2006), by employing a thin test surface having low heat capacity. However, the major problem of these measurements is attenuation of the temperature fluctuation due to the heat capacity of the test surface. Also, lateral conduction through the test surface attenuates the amplitude of the spatial temperature distribution. These attenuations are considerably large, especially for the heat transfer to air for which the heat transfer coefficient is low.

The present author investigated the frequency response and the space resolution of the heat transfer from a test surface by solving heat conduction equations (Nakamura, 2007). Figure 1 (a) and (b) shows the upper limit of the fluctuating frequency, f_{max}, and the lower limit of the spatial wavelength, b_{min}, respectively, which are detectable using infrared thermograph, where Δh is fluctuating amplitude of the heat transfer coefficient and ΔT_{IR0} is noise equivalent temperature difference (NETD) of infrared thermograph for a black body. If an extremely thin conductive film, as indicated in Fig. 1, is used as the heated surface, the unsteady heat transfer to air is observable up to $f \approx$ 50 Hz and $b \approx$ 1 mm (at $T_w - T_0$ = 30°C and Δh = 3 – 5 W/m^{2}K) by employing an infrared thermograph of nowadays (ΔT_{IR0} = 0.025°C).

In this work, the measurement technique using a thin conductive film and a high-speed infrared thermograph was applied to measure the unsteady heat transfer to air caused by flow turbulence. The attenuation due to the heat capacity and the lateral conduction was restored by solving the heat conduction equations inside the wall.

NOMENCLATURE

b_c : cutoff wavelength in space
b_{min} : lower limit of spatial wavelength detectable
c : specific heat
f_c : cutoff frequency
f_{max} : upper limit of fluctuating frequency detectable
h : heat transfer coefficient
l_τ : wall-friction length = ν/u_τ
$\dot{q}$: heat flux
Re_θ : Reynolds number based on momentum thickness
T : temperature
T_0, T_w : freestream and wall temperatures
ΔT_{IR0} : noise equivalent temperature difference of infrared thermograph for a black body
t : time
u_0, u_τ : freestream and wall-friction velocities
x, y, z : streamwise, vertical, and spanwise coordinates
δ : thickness
λ : thermal conductivity
ν : kinematic viscosity of fluid
ρ : density of fluid

Superscripts and Subscripts
$(^-)$: mean value
$()_{rms}$: root-mean-square value
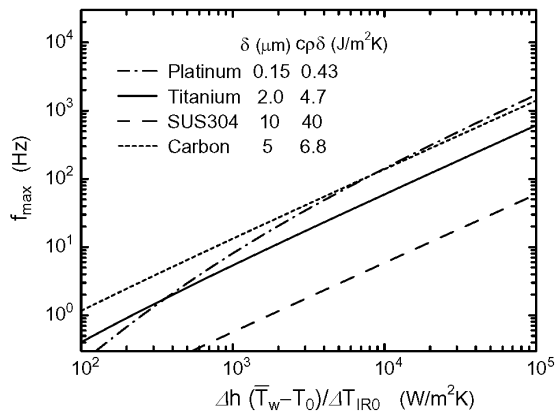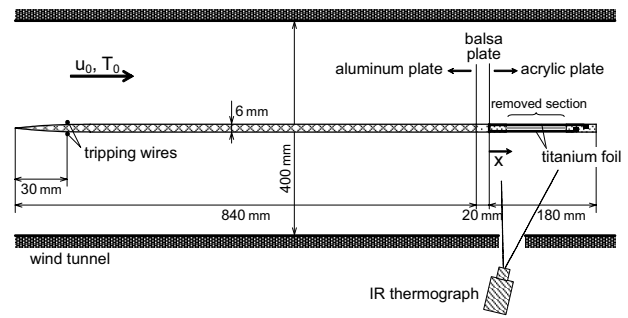
(a) Upper limit of the fluctuating frequency
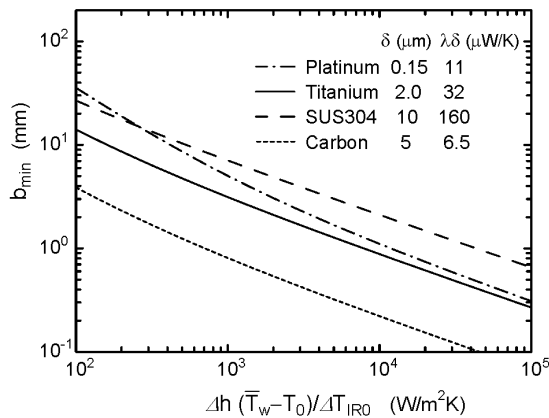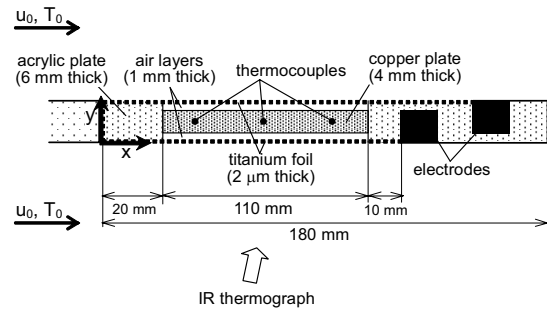

(b) Lower limit of the spatial wavelength

Fig. 1 Limits of the fluctuating frequency and the spatial wavelength detectable using infrared measurements.

(a) Cross-sectional view of the wind tunnel

(b) Cross sectional view of the acrylic plate

(c) Photograph of the acrylic plate

Fig. 2 Test plate used in this study.
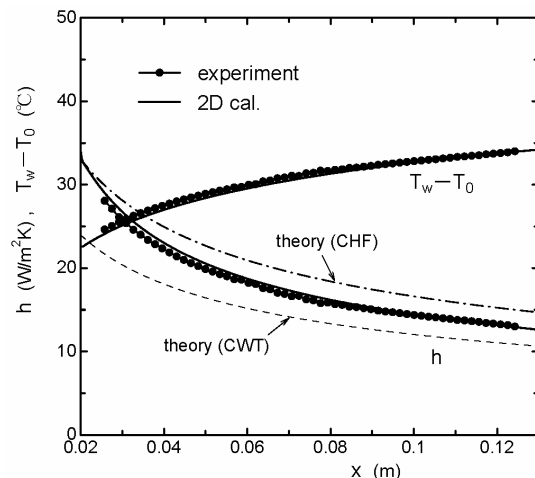
Fig. 3 Streamwise distribution of h and T_w-T_0 for laminar boundary layer at $u_0 = 4$ m/s.
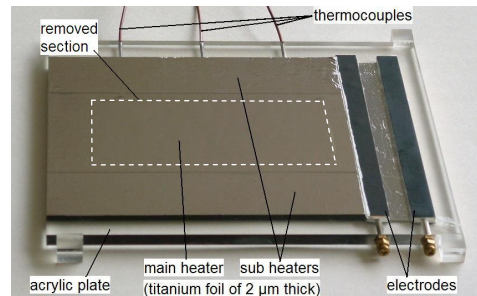
EXPERIMENTAL APPARATUS

The measurements were preformed using a flat plate placed in a wind tunnel, as shown in Fig. 2. The test plate (6 mm thick) had a removed section, which was covered with a titanium foil of 2 μm thick on both the lower and upper faces. A copper plate of 4 mm thick was placed at the mid-height of the removed section, as shown in Fig. 2 (b). The titanium foil was heated by applying a direct current under conditions of constant heat flux so that the temperature difference between the foil and the freestream was about 30°C. Under these conditions, air enclosed by both the titanium foil and the copper plate does not convect because the Rayleigh number is below the critical value. This insulates most of the heat conduction loss to inside the plate, and thus retains the fluctuations and the spatial distribution of the temperature on the titanium foil, as reflected by unsteady heat transfer to outside the plate. The mechanical vibration of the titanium foil caused by the unsteadiness in the flow was less than 10 μm in amplitude, which was much smaller than the wall-friction length $l_\tau = \nu/u_\tau$. The infrared thermograph was positioned below the plate and it measured the fluctuation of the temperature distribution on the lower-side face of the plate through a hole drilled in the lower wall of the wind tunnel. The infrared thermograph

(a) Laminar boundary layer at $u_0 = 3$ m/s; left – instantaneous distribution, right – time trace at $x = 37$ mm

(b) Turbulent boundary layer at $u_0 = 3$ m/s, $Re_\theta = 530$, $l_\tau = 0.126$ mm;
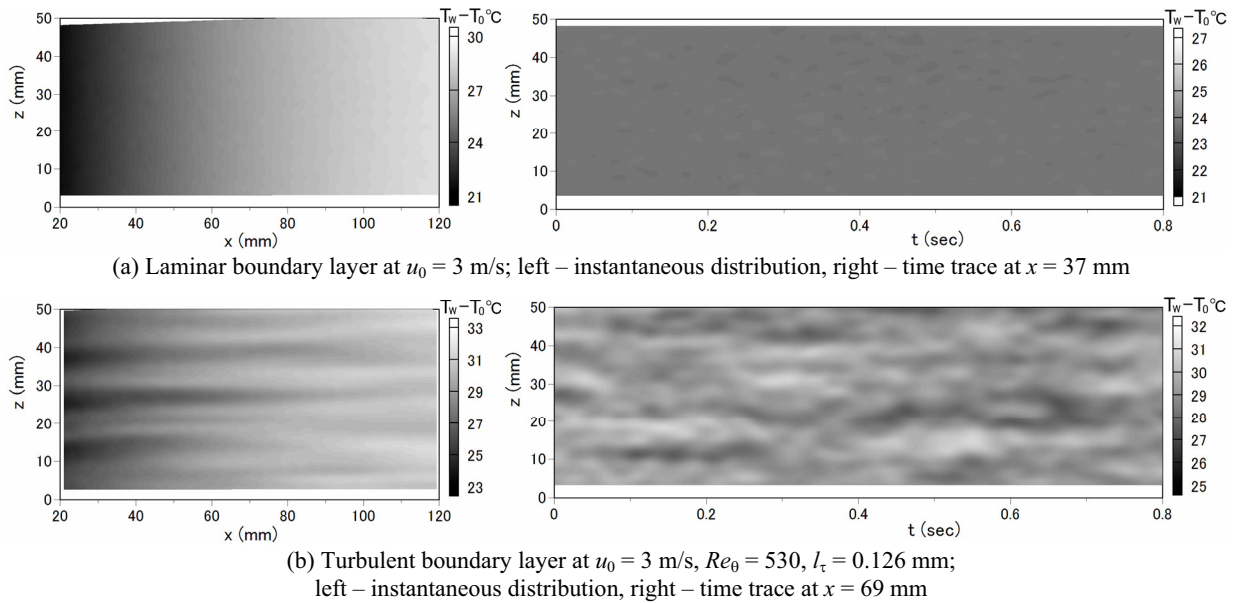left – instantaneous distribution, right – time trace at $x = 69$ mm

Fig. 4 Temperature distribution $T_w - T_0$ on the titanium foil measured using infrared thermography.

used in this study (TVS-8502, Avio) can capture images of the instantaneous temperature distribution at 120 frames per second, and a total of 1024 frames with a full resolution of 256×236 pixels. The value of NETD (noise equivalent temperature difference) of the infrared thermograph for a black body was 0.025°C. The effect of diffuse reflection from the surroundings was suppressed by coating the inner surface of the wind tunnel with black paint.

RESULTS

Accuracy Verification

Figure 3 shows streamwise distribution of the heat transfer coefficient, h, together with the temperature difference between the titanium foil and the freestream, $T_w - T_0$, measured using infrared thermography under conditions of a laminar boundary layer. Solid lines show the result of a 2D heat conduction analysis performed by assuming the velocity distribution to be a theoretical value. The agreement between the experimental and the analytical values are very well (within 3 %), indicating that the present measurements lead to a reliable heat transfer coefficient at least for a steady flow condition.

A dynamic response of the temperature on the heated surface was evaluated experimentally against a stepwise change of the heat input to the foil in conditions for a laminar boundary layer. The result showed a good agreement to that of the heat conduction analysis.

Measurements for Turbulent Boundary Layer

A turbulent boundary layer was generated by attaching 2 mm diameter tripping wires to both the lower and upper faces of the flat plate, as shown in Fig. 2 (a), at a position 30 mm from the leading edge of the plate. The distance from the tripping wire to the leading edge of the titanium foil ($x =$

0) was 830 mm. The velocity distribution in the turbulent boundary layer was measured using hot-wire and cold-wire probes. The mean velocity distribution corresponded well to the experimental data obtained by Klebanoff (1955), and the rms value agrees fairly well to the experimental data (Klebanoff, 1955) and DNS of Spalart (1988).

Figure 4 (a) and (b) shows the results of the temperature distribution on the wall of laminar and turbulent boundary layers, respectively, measured using infrared thermography. The freestream velocity was $u_0 = 3$ m/s for both cases. For the turbulent boundary layer, Reynolds number based on the momentum thickness was $Re_\theta = 530$ at $x = 100$ mm, at which the wall-friction velocity and the wall-friction length were respectively $u_\tau = \sqrt{\nu \left| \partial \overline{u} / \partial y \right|} = 0.139$ m/s and $l_\tau = \nu / u_\tau = 0.126$ mm. Bad pixels existed in the thermo-images were removed by applying a 3×3 median filter. Also, a sharp cut-off filter was applied in order to remove a high frequency noise more than 30 Hz (corresponds to 4 frames) and the small-scale spatial noise less than 3.4 mm (corresponds to 6 pixels). The effect of nonuniformity in the thickness of the titanium foil was corrected in the same manner as described by Nakamura and Igarashi (2006). However, the correction was very small, about 0.3 % of $T_w - T_0$ in rms value, due to an excellent uniformity in the thickness of the titanium foil used herein.

As depicted in Fig. 4 (b), the turbulent boundary layer has large fluctuation and nonuniformity in temperature according to the flow turbulence. The thermal streaks appear in the instantaneous distribution, which extend to the streamwise direction. Figure 5 shows the power spectrum of the temperature fluctuation. The SN ratio of the measurement based on the power spectrum for the laminar boundary layer was 500 – 1000 (27 – 30 dB) in the lower frequency range of 0.4 – 6 Hz by applying the sharp cut-off filter. Figure 6 shows the two-point correlation of the spanwise temperature distribution. For the turbulent

boundary layer, the correlation has a minimum value at $\Delta z = 6.8$ mm, indicating a periodicity in the thermal streaks in the spanwise direction. In contrast, the value for the laminar boundary layer is negligibly small except for small-scale noise at $\Delta z < 1.6$ mm, most of which disappears by applying the sharp cut-off filter.

Restoration of Heat Transfer Coefficient

The local and instantaneous heat transfer coefficient was calculated using the following equation derived from the heat conduction equation in a thin conductive film.

$$h = \frac{\dot{q}_{in} - \dot{q}_{cd} - \dot{q}_{rd} - \dot{q}_{rdi} + \lambda\delta\left(\dfrac{d^2T_w}{dx^2} + \dfrac{d^2T_w}{dz^2}\right) - c\rho\delta\dfrac{dT_w}{dt}}{T_w - T_0} \quad (1)$$

This equation contains both terms of lateral conduction through a conductive film, $\lambda\delta(\, d^2T_w/dx^2 + d^2T_w/dz^2\,)$, and the delay due to the heat capacity of the film, $c\rho\delta(\, dT_w/dt\,)$. Here, c, ρ, δ and λ are specific heat, density, thickness and thermal conductivity of the titanium foil, respectively. $\dot{q}_{in}$ is the input heat-flux to the titanium foil, $\dot{q}_{rd}$ and $\dot{q}_{rdi}$ are radiation heat fluxes to the outside and inside the test plate, respectively. Heat conduction to the air layer, $\dot{q}_{cd} = -\lambda_a\,(dT/dy)$, can be determined by solving the heat conduction equation in the air layer, which is enclosed between the titanium foil and the copper plate.

$$c_a\rho_a\frac{dT}{dt} = \lambda_a\left(\frac{d^2T}{dx^2} + \frac{d^2T}{dy^2} + \frac{d^2T}{dz^2}\right) \quad (2)$$

Here, c_a, ρ_a and λ_a are specific heat, density and thermal conductivity of air. Since the temperature of the copper plate is assumed to be steady and uniform, the boundary condition of Eq. (2) on the copper plate side can be applied by a mean temperature of the copper plate measured using thermocouples.

The finite difference method was used to calculate the heat transfer coefficient h from Eq. (1) and (2). Time differential dt was set to 0.0083 sec, which corresponds to the frame interval of the thermo-images. Space differentials dx and dz were set to 0.58 mm and 0.54 mm, respectively, corresponding to the pixel pitch of the thermo-image. The thickness of the air layer ($\delta_a = 1$ mm) was divided into two regions ($dy = 0.5$ mm). Eq. (2) was solved using ADI (alternative direction implicit) method (Peaceman and Rachford, 1955) with respect to x and z directions.

The above procedure of the finite different method, which included the effects of the median filter and the sharp cut-off filter, restored the heat transfer coefficient up to $f_c = 30$ Hz in time (corresponding to four frames) and $b_c = 4.5$ mm in spatial wavelength (corresponding to eight pixels), with the attenuation rate of below 20 %. The wavelength of $b_c = 4.5$ mm corresponded to $26 - 66\ l_\tau$ (for $u_0 = 2 - 6$ m/s), which was smaller than the mean distance between the thermal streaks ($\approx 100\ l_\tau$, see Fig. 10).

Figure 7 shows cumulative power spectrum of the velocity fluctuation in the near-wall region ($y^+ = 10$) of the turbulent boundary layer. For $u_0 = 2$ m/s, the fluctuation energy below $f_c = 30$ Hz accounts for 92 % of the total energy. In this case, the fluctuating heat transfer can be
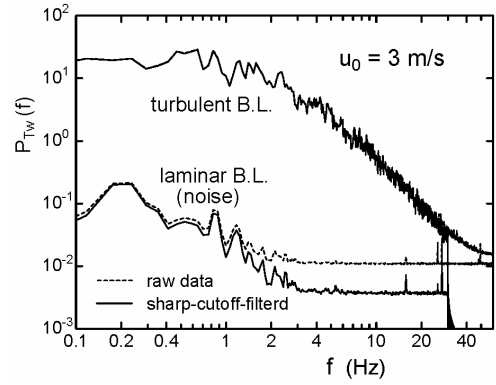

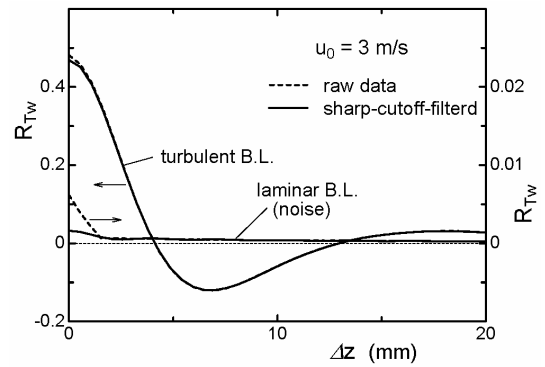Fig. 5 Power spectrum of the temperature fluctuation

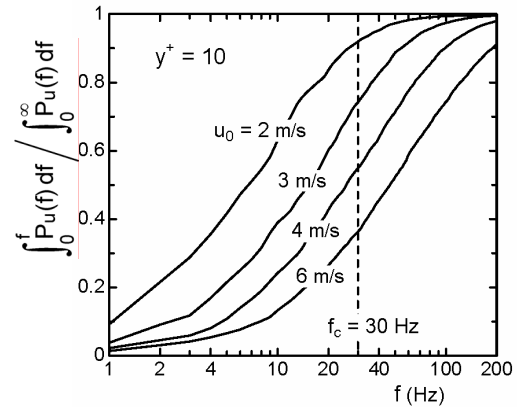Fig. 6 Two-point correlation of spanwise temperature distribution.

Fig. 7 Cumulative power spectrum of the velocity fluctuation in the turbulent boundary layer at $y^+ = 10$.

restored almost completely using the above procedure. However, with an increase in the freestream velocity, the ratio of the fluctuation energy below $f_c = 30$ Hz decreases, resulting in an insufficient restoration.

Time-Space Distribution of Heat Transfer

The time-space distribution of the heat transfer coefficient restored using the above procedure is shown in Fig. 8. The features of the thermal streaks are clearly

(a) $u_0 = 2$ m/s, $Re_\theta = 280$, $l_\tau = 0.174$ mm; left – instantaneous distribution, right – time trace at $x = 69$ mm

(b) $u_0 = 3$ m/s, $Re_\theta = 530$, $l_\tau = 0.126$ mm; left – instantaneous distribution, right – time trace at $x = 69$ mm
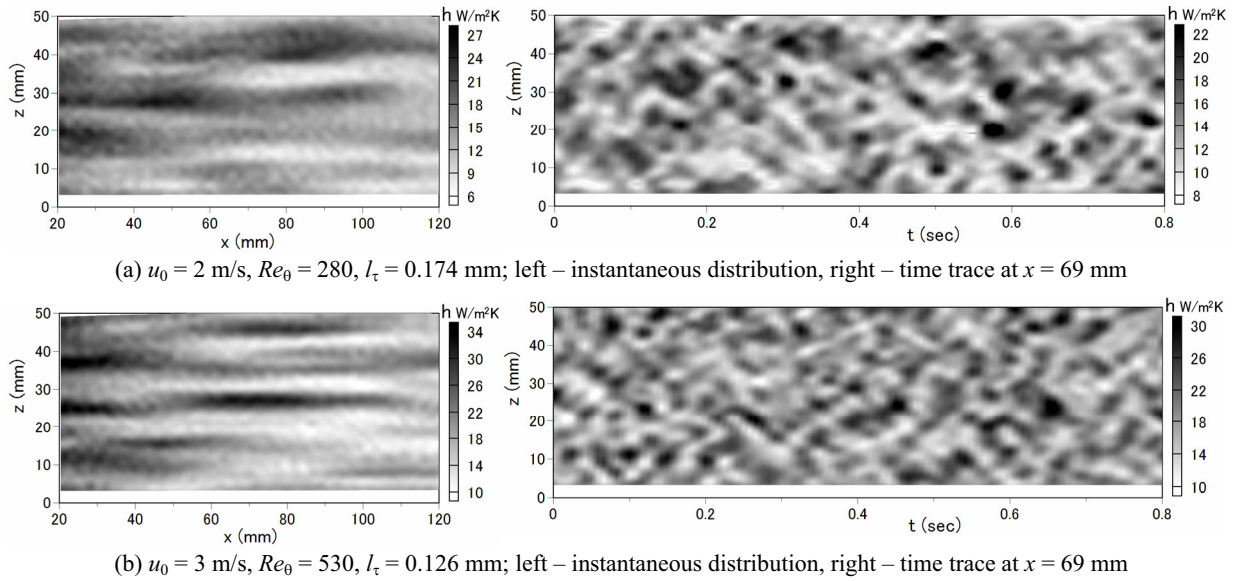
Fig. 8 Time-spatial distribution of heat transfer coefficient on the wall of a turbulent boundary layer.

revealed, which extend to the streamwise direction with small spanwise inclinations. The heat transfer coefficient fluctuates vigorously showing a quasi-periodic characteristic in both time and spanwise wavelength, which is reflected by the unique behavior of the thermal streaks. Although the restoration for $u_0 = 3$ m/s (Fig. 8 (b)) is not sufficient, as shown in Fig. 7, the characteristic scale of the fluctuation seems to be smaller both in time and spanwise wavelength than that for $u_0 = 2$ m/s, indicating that the structure of the thermal streaks becomes finer with increasing the freestream velocity.

Figure 9 plots the rms value of the fluctuation $h_{rms}/\bar{h}$ at $x = 69$ mm. The value was $h_{rms}/\bar{h} = 0.23$ at $u_0 = 2$ m/s ($Re_\theta = 280$), at which the restoration is almost complete. However, it decreases with increasing the freestream velocity due to the insufficient restoration. For $u_0 = 2$ m/s, the upper limit of the fluctuating frequency detectable using the infrared thermography is $f_{max} = 37$ Hz (see Fig. 1 (a)), while the restored frequency is $f_c = 30$ Hz. This means that the restoration is possible up to $f_c \approx f_{max}$ without a considerable increase in noise.

The results of DNS (Lu and Hetsroni, 1995, Kong et al, 2000, Tiselj et al, 2001, and Abe et al, 2004) are also plotted in Fig. 9. As shown in this Figure, the value of $h_{rms}/\bar{h}$ greatly depends on the difference in the thermal boundary condition, that is, $h_{rms}/\bar{h} \approx 0.4$ for steady temperature condition (corresponds to infinite heat capacity wall), whereas $h_{rms}/\bar{h} = 0.13 - 0.14$ for steady heat flux condition (corresponds to zero heat capacity wall). Since the present experiment was performed between two extreme conditions, for which the temperature on the wall fluctuates with a considerable attenuation, the value $h_{rms}/\bar{h} = 0.23$ seems to be reasonable.

Figure 10 plots the mean spanwise wavelength of the thermal streak, $l_z^+ = l_z/l_\tau$, which is determined by the two-point correlation of the heat transfer coefficient. For the lower velocity of $u_0 = 2 - 3$ m/s ($Re_\theta = 280 - 530$), the mean
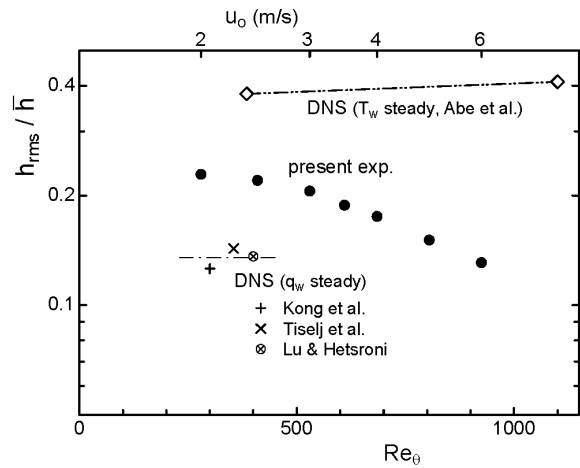

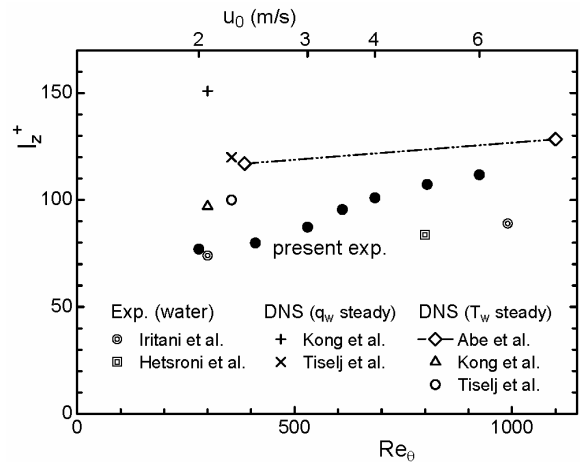Fig. 9 Rms value of the fluctuation heat transfer coefficient.

Fig. 10 Mean spacing of thermal streaks

wavelength is $l_z^+ = 77 - 87$, which agrees well to that for the previous experimental data obtained using water as a working fluid (Iritani et al, 1983 and 1985, and Hetsroni and Rozenblit, 1994, $l_z^+ = 74 - 89$). This wavelength is smaller than that for DNS (Kong et al, 2000, Tiselj et al, 2001, and Abe et al, 2004, $l_z^+ = 100 - 150$), probably due to the additional flow turbulence in the experiments, such as freestream turbulence. The value of l_z^+ increases with increasing the freestream velocity u_0, probably due to fact that the streaks of short-duration (lower than 1/30 sec) were not restored in this experiment.

In this work, the time-space distribution was restored up to 30 Hz in time and 4.5 mm in spatial wavelength at a low heat transfer coefficient of $\bar{h} = 10 - 20$ W/m²K, by employing a 2 μm thick titanium foil and an infrared thermograph of 120 Hz with a full resolution of 256×236 pixels. This restoration was, however, not exactly sufficient, particularly for the higher freestream velocity of $u_0 > 2$ m/s. If we employ the higher-grade product of infrared thermograph (420 Hz with a full resolution of 640×512 pixels and with a NETD of 0.025°C), it will be possible to restore up to $f_c = 105$ Hz (corresponding to 4 frames) in time and $b_c = 1 - 2$ mm or less in space (corresponding to 8 pixels), within the conditions of $f_c < f_{max}$ and $b_c > b_{min}$. This seems that this technique is promising to study the time-space behavior of the heat transfer to air caused by flow turbulence. The finer structure in time and space can be restored in the future, depending on the improvements of both the performance of the thermograph and the quality of the thin conductive film.

CONCLUSION

A measurement technique using a thin conductive film and a high-speed infrared thermograph was applied to measure the time-space distribution of heat transfer to air on the wall of a turbulent boundary layer. In this work, a titanium foil of 2 μm thick was used as a heated surface, and measured temperature on it by employing an infrared thermograph of 120 Hz. Measurements were performed by using a test plate consisted of three layers, that is, the titanium foil heated electrically, a stationary air layer, and a copper plate. The time-space distribution of the heat transfer coefficient was restored up to 30 Hz in time (corresponding to four frames of the thermo-images) and 4.5 mm in spatial wavelength (corresponding to eight pixels of the thermo-image) at low heat transfer coefficient of $\bar{h} = 10 - 20$ W/m²K, by solving the heat conduction equation in both the titanium foil and the air layer. The results showed that the time-space behavior of the heat transfer was clearly revealed, which was reflected by the streaks formed in the near-wall region of the turbulent boundary layer. The fluctuation of the heat transfer coefficient was $h_{rms}/\bar{h} = 0.23$ at $Re_\theta = 280$ ($u_0 = 2$ m/s), which was reasonable compared to the results of DNS. Also, mean spacing of the thermal streaks at $Re_\theta = 280 - 530$ was $l_z^+ = 77 - 87$, which

agreed well to the previous experiments using water as a working fluid. These results support that this technique is promising to study the heat transfer to air caused by flow turbulence.

REFERENCES

Abe, H., Kawamura, H. and Matsuo, Y., 2004, "Surface Heat-Flux Fluctuations in a Turbulent Channel Flow up to $Re_\tau = 1020$ with Pr = 0.025 and 0.71", Int. J. Heat and Fluid Flow, Vol. 25, pp. 404-419.

Iritani, Y., Kasagi, N., and Hirata, M., 1983, "Heat Transfer Mechanism and Associated Turbulent Structure in the Near-Wall Region of a Turbulent Boundary Layer", *4th Symposium on Turbulent Shear Flows*, pp. 17.31-17.36.

Iritani, Y., Kasagi, N. and Hirata, M., 1985, "Streaky Structure in a Two-Dimensional Turbulent Channel Flow" (in Japanese), Trans. Jpn. Soc. Mech. Eng., Vol. 51, No. 470, B, pp. 3092-3101.

Hetsroni, G., and Rozenblit, R., 1994, "Heat Transfer to a Liquid-Solid Mixture in a Flume", Int. J. Multiphase Flow, Vol. 20, No. 4, pp. 671-689.

Klebanoff, P.S., 1955, "Characteristics of Turbulence in a Boundary Layer with Zero Pressure Gradient", *NACA Rep.* 1247.

Kong, H., Choi, H. and Lee, J.S., 2000, "Direct Numerical Simulation of Turbulent Thermal Boundary Layers", Physics of Fluids, Vol. 12, No. 10, pp. 2555-2568.

Lu, D.M. and Hetsroni, G., 1995, "Direct Numerical Simulation of a Turbulent Open Channel Flow with Passive Heat Transfer", Int. J. Heat and Mass Transfer, Vol. 38, No. 17, pp. 3241-3251.

Nakamura, H., and Igarashi, T., 2004, "Unsteady heat transfer from a circular cylinder for Reynolds numbers from 3000 to 15000", Int. J. Heat and Fluid Flow, Vol. 25, pp. 741-748.

Nakamura, H., and Igarashi, T., 2006, "A New Technique for Measurements of Unsteady Heat Transfer to Air Using a Thin Metallic-Foil and Infrared Thermograph", 13th Int. Heat Transfer Conf., EXP-11, Sydney, Australia.

Nakamura, H., 2007, "Frequency-Response and Space-Resolution for Measurements of Convective Heat Transfer Using a Thin Conductive Film", Trans. Jpn. Soc. Mech. Eng. (in Japanese), Vol. 69, No. 681, B, pp. 601-609.

Peaceman, D.W. and Rachford, H.H., 1955, "The numerical solution of parabolic and elliptic differential equations", J. Soc. Ind. Appl. Math., Vol.3, pp.28-41.

Spalart, P.R., 1988, "Direct Simulation of a Turbulent Boundary Layer up to $Re_\theta = 1410$", J. Fluid Mech., Vol. 187, pp .61-98

Tiselj, I., Pogrebnyak, E., Li, C., Mosyak, A., and Hetsroni, G., 2001, "Effect of Wall Boundary Condition on Scalar Transfer in a Fully Developed Turbulent Flume", Physics Fluids, Vol. 13, No. 4, pp. 1028-1039.